C.P. No. 775

C.P. No. 775

MINISTRY OF AVIATION

AERONAUTICAL RESEARCH COUNCIL

CURRENT PAPERS

Low-Speed Wind-Tunnel Tests on a Series of Cambered Ogee Wings

by

P. B. Earnshaw

LONDON: HER MAJESTY'S STATIONERY OFFICE

1964

PRICE 5s 6d NET

R29307

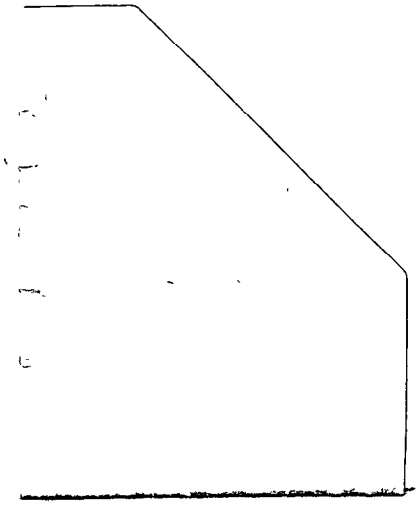

U.D.C. No. 533.6.055 : 533.6.071 : 533.693.4

C.P. No.775
November 1963

LOW-SPEED WIND-TUNNEL TESTS ON A SERIES OF CAMBERED OGEE WINGS

by

P. B. Earnshaw

SUMMARY

A series of nine cambered ogee models, each having the same planform and area distribution, has been tested at low speeds. The camber variants have been designed by means of slender-wing theory and include variations both of lift coefficient for attached flow and of pitching moment at a given lift. For all wings, the flow development was regular regardless of load distribution except at low incidences, where the flow was very sensitive to defects in the leading edges. Trailing-edge effects dominated the load distribution achieved in the attachment condition; when an appreciable part of the load was carried over the forward part of the wing, correspondence between theory and experiment was reasonable. Increase of lift coefficient for attached flow had favourable effects with regard to both $(L/D)_{max}$ and the rate of forward movement of aerodynamic centre with increasing lift.

Replaces R.A.E. Tech. Note No. Aero 2928 - A.R.C. 25736.

CONTENTS

ILLUSTRATIONS

1 INTRODUCTION

Longitudinal camber designed into the wing can produce a trimmed condition at cruise on a supersonic transport aircraft for smaller drag penalty than by use of elevators[1]. But, whilst it is known that the slender-wing theory is capable of producing camber shapes having attached flow at the design incidence, experimental results for a wide range of such designs are desirable in order to investigate any limitations which could preclude regular vortex development off-design or indeed any limitations to the theory itself. Such limitations might exist, for example, with respect to maximum permitted droop angle or rate of change of droop angle along the leading edge, or to the thickness effects of a practical area distribution which might become restrictive in the forward part of the wing. Equally, of course, it is necessary to determine the extent to which such factors influence the actual load distributions compared with those predicted by the theory.

The basis for the present work was the planform and thickness distribution resulting from a feasibility study completed in 1960. Owing to the comparative ease of manufacture of small wooden models for the R.A.E. 4 ft × 3 ft low-speed wind tunnel, an extensive series of cambered designs has been tested there during mid 1960 in order to cover as wide a range of parameters as possible. The choice of designs may be broadly divided into two groups - forward and rearward variations. At supersonic speeds, some load distributions at the front of the aircraft may be helpful in reducing wave drag due to lift while still attaining a given pitching moment; but, due to the excessive thickness and rate of change of span, might lead to uneven flow development at low speed and high incidence. The rear part of the wing is affected mainly by change of design lift coefficient which can be expected to influence the maximum lift/drag ratio as well as the maximum practical lift coefficient which can be used for landing. At low speeds the trailing-edge effects, not considered in slender-wing theory, will also play a large part in this area of the wing. The series of measurements of lift, drag and pitching moment together with surface flow patterns reported in this Note help to clarify some of these points.

2 DETAILS OF MODELS AND TESTS

Nine models have been tested, each having the same ogee planform with $p = 0.45$ and the same area distribution which corresponds very closely with that chosen for models 15, 16, 17, 18 of the 8 ft × 8 ft supersonic tunnel programme[2].

The camber surfaces for these wings have been computed using the downwash distribution given by

$$-\frac{\partial z}{\partial x} = C(x) \qquad \text{for } 0 \leq |\eta| \leq \eta_o(x)$$

$$= C(x)\left[1 - \frac{\pi(|\eta| - \eta_o)^2}{(1 + 2\eta_o^2)\cos^{-1}\eta_o - 3\eta_o\sqrt{1 - \eta_o^2}}\right] \qquad \text{for } \eta_o(x) \leq |\eta| \leq 1$$

shown by Weber[3] to include the condition for attachment. Adding to this distribution the condition that the trailing edge is straight, the camber surface is designed for any given centre-line slope. The uncambered model of the present series corresponds with model 15 of the 8 ft × 8 ft supersonic tunnel programme, while models 1, 2 of the present series correspond with models 15, 16 of that programme except in that the latter have been designed to have the section at 95% length uncambered, rather than the trailing edge itself. Local load distributions and leading-edge droop distributions are shown in Figs.3(a), 3(b), 4(a) and 4(b).

Models 1, 3, 4, 8 comprise a set of designs each having zero load over the forward 20% of the wing. The design C_L increases in equal increments from 0 to 0.075 while the corresponding ΔC_m, which is defined as the pitching moment of the cambered wing minus the pitching moment of the plane wing of the same planform at the design C_L, decreases in equal increments from 0.0085 to 0.0030. Model 2, which is the only design having a finite load at the trailing edge, has been designed for a C_L of 0.025 and, by allowing droop angles of up to 50°, carries more load forward in order to reduce wave drag due to lift at supersonic speeds. Model 5 has the same load and therefore droop-angle distribution at the front of the wing but the rear part of the wing is such as to give zero design C_L. It was hoped that model 5 would help in interpretation of any peculiarities which might arise in Model 2. Model 7 results from a combination of the ordinates of models 1 and 5 in such a manner as to produce a maximum droop angle of 60°. Model 6 has the same load distribution as model 5 over the rear part of the wing but the droop angle is made finite at the apex, thus producing a finite rate of growth of load at the apex and carrying rather more load forward.

These models were tested in the 4 ft × 3 ft low-turbulence wind tunnel, using a standard wire rig, over an incidence range of -4° to 24° where the design incidence for each model is regarded as zero. A wind speed of 200 ft/sec was used throughout except at the highest incidences where intense vibration of the models necessitated a drop to 100 ft/sec. Measurements were made of lift, drag and pitching moment. Surface flow patterns were produced using a mixture of lamp black and paraffin, the models being sting mounted for this purpose and a wind speed of 100 ft/sec being used. Each model has been tested both smooth and with transition wires on the upper surface. The latter took the form of a semi-circular wire (26 S.W.G.) on the upper surface of the nose, approximately 10% centre-line chord behind the apex, together with a wire (32 S.W.G.), approximately 10% local semi-span inboard of each leading edge. These transition wires were designed to eliminate the separations occurring inboard of the shoulder lines over the rear part of the wing at incidences close to that for attached flow at the leading edge. These separations were so serious that all the results plotted are those produced with transition wires attached to the model.

Tunnel constraint corrections, applied to the force measurements, allow for the slenderness of the models by the technique described by Berndt[4], who uses slender-body theory everywhere except in the drag correction. Unfortunately there is an apparent conflict between the value for the drag correction obtained by the application of slender-body theory to the conditions at the

trailing edge and that obtained by Berndt using Munk's stagger theorem which equates the interference drag from a lifting surface to that due to a lifting line and which therefore predicts the same drag correction irrespective of slenderness. As it has not yet been found possible to resolve the conflict, the slender-body correction has been used for all components simply on the grounds of consistency. In this instance, the difference between the drag corrections amounts, at maximum C_L, to only 0.5% of total drag.

3 DISCUSSION OF RESULTS.

3.1 Force measurements

Figs.5(a), (b) show that as expected the lift curves are all essentially parallel, each being displaced by the C_L achieved at design incidence. This achieved C_L does not correspond well with C_{L_D} (i.e. the design C_L) but the differences can be explained at least qualitatively in terms of the subsonic trailing-edge effects. Marked on each curve is the incidence at which a line joining the trailing edge to a point 70% chord from the apex, makes an angle of 15° with the horizontal. This gives some indication of the restriction which undercarriage length would place on landing attitude. These points demonstrate that on this basis, designing for a higher C_{L_D} results in a loss of C_L for landing. However, each of these wings is convex towards the ground on the rear part of the wing. It does not follow therefore that this effect holds true in other cases.

Owing to the fairly high incidence range covered and consequently the need for heavy rigging wires, the accuracy of drag measurements at low incidence leaves much to be desired. However, the curves of variation of induced drag factor, K, with lift (Fig.6) show a clear trend at low C_L, namely that an increase in C_{L_D} produces a reduction in K. The curves of induced drag factor, K_s, based on the minimum drag for the symmetrical wing do not disturb this trend (Fig.7) except in the case of model 8 where the minimum drag has risen to such a level as to produce a minimum of K_s in the neighbourhood of $C_L = 0.15$. This effect is reflected also in the value of $(L/D)_{max}$; see Figs.8(a), (b) and Table 1. This indicates that $(L/D)_{max}$ increases with increasing C_{L_D} at least until $C_{L_D} = 0.075$ but the trend suggests that further increases, if any, will be small. At higher values of C_L, two general trends of the induced drag factors can be distinguished: (a) an increase in C_{L_D} produces a decrease in K; (b) more extreme camber distributions produce increases in K. Thus the symmetrical model has a lower value of K than the highly cambered model 2 but greater than model 3 although both have the same C_{L_D}.

Pitching moments are plotted in Fig.9. As non-linear lift is not appreciable for C_L's up to about 0.05, it seems not unreasonable to compare the achieved ΔC_m with the theoretical value at zero lift rather than at design

incidence. Comparison of the values shown in Table 1 demonstrates that where a large part of the camber loading is carried over the forward part of the wing, a greater proportion of the theoretical ΔC_m is achieved. Again this offers support for the suggestion that trailing-edge effects dominate any changes in the theoretical loading due to camber. Model 2 is perhaps a special case with regard to this argument, as the theoretical finite load at the trailing edge could not be recovered in subsonic flow, thus resulting in much closer agreement of theoretical ΔC_m with experiment than in other cases.

All the pitching-moment curves show waviness in the neighbourhood of C_{L_D} and at higher C_L's, most of the curves display "flats". Unfortunately there are insufficient experimental points to determine these accurately but, as most of the curves show these features, it seems certain that they do exist at least at this Reynolds number. However, in order to produce the curves showing variation of aerodynamic centre with lift (Fig.10(a), (b)) smoothed pitching-moment curves have been used. Here again the effects of increasing C_{L_D} and of introducing more extreme camber distributions appear to produce conflicting trends, namely that the addition of camber increases the forward movement of the aerodynamic centre while increase of C_{L_D} reduces it.

3.2 Surface flow patterns

Surface flow patterns produced by a suspension of lamp black in kerosine show in Fig.11(a) the extensive laminar separations occurring at the shoulder lines at the design incidence. These separations are present to a greater or lesser degree on all the cambered models. However, the use of transition wires as shown in Fig.11(b) completely eliminates this problem, and results in an increase in $C_{D_{min}}$, for example from 0.0072 to 0.0085 on model 4.

At low incidence when the leading-edge vortex is weak, the flow develops in an irregular manner at the leading edge resulting in what are apparently streamwise vortices, as shown in Fig.12(a) for 2.5° above design incidence. All of the fairly well defined traces on this and on other models could be seen to originate at barely perceptible defects in the leading edges. On increasing the incidence these traces disappeared, so that at 5° only those due to relatively serious defects remained, while at 10° the flow pattern was developing quite smoothly (see Fig.12(b)) and did not change in character up to the maximum incidence of 25°. The sensitivity of the flow at low incidences to small irregularities in shape at the leading edge must be attributed to the combination of planform and thickness distribution of this series of models. Camber, within the range tested, had no evident effect on the regularity of flow development.

In the neighbourhood of the apex, the flow remained attached at the leading edges but, in this region, difficulties of model manufacture ensure that the leading edge is by no means sharp so that this feature might well be expected.

4 CONCLUSIONS

On all of the wings tested the flow development became regular above some incidence between 5° and 10°. At lower incidences, the flow was very sensitive

to the smoothness of the leading edge where very small defects in a model could give rise to noticeable disturbances downstream. This sensitivity did not appear to be influenced by the camber distribution.

The difference between the load distribution achieved and that predicted by slender-wing theory seemed to be dominated by trailing-edge effects, and agreement with design values was good only when an appreciable part of the load was carried over the forward part of the wing. The introduction of camber in order to produce a given pitching moment resulted also in an increase of induced drag and consequently a reduction in $(L/D)_{max}$. An increase in design lift coefficient C_{L_D} was more favourable in increasing $(L/D)_{max}$ as well as reducing the increased rate of forward movement of aerodynamic centre produced by the addition of camber. A less favourable characteristic was the reduction in attainable C_L for landing.

SYMBOLS

A	aspect ratio
c_o	centre-line chord
$\bar{\bar{c}}$	aerodynamic mean chord
$C(x)$	downwash at centre section of camber surface
C_L, C_D	coefficients of lift and drag
C_m	pitching moment coefficient taken about $0.66\ c_o$ and referred to $\bar{\bar{c}}$
$C_{D_{min}}$	minimum drag coefficient
$C_{D_{sym}}$	minimum drag coefficient of symmetrical wing
C_{L_D}	design lift coefficient
K	$= \dfrac{C_D - C_{D_{min}}}{C_L^2/\pi A}$, induced drag factor
K_s	$= \dfrac{C_D - C_{D_{sym}}}{C_L^2/\pi A}$, induced drag factor based on symmetrical wing drag
$L(x)$	cross load
$s(x)$	local semi-span

SYMBOLS (CONTD)

s_T	semi-span at trailing edge
$S(x)$	cross-sectional area distribution
v	total volume
x,y,z	Cartesian coordinates; origin at the wing apex; x along the free stream direction, y spanwise, z positive upwards; all lengths made dimensionless with the root chord
δ	leading edge droop angle in cross-plane
η	$= \frac{y}{s(x)}$, non-dimensional spanwise ordinate
η_o	non-dimensional spanwise position of "shoulder"

REFERENCES

No.	Author	Title, etc
1	Richardson, J.R.	Supersonic trim drag of delta wings. Handley Page Ltd. HP/Aero/300. Aug. 1957.
2	Taylor, C.R.	Measurements at Mach numbers up to 2.8 of the longitudinal characteristics of one plane and three cambered slender ogee wings. ARC R & M 3328. December 1961.
3	Weber, J.	Design of warped slender wings with the attachment line along the leading edge. ARC 20051. September 1957.
4	Berndt, S.B.	Wind tunnel interference due to lift for delta wings of small aspect ratio. Kungl. Tekniska Högskolan KTH - Aero TN 19. September, 1950.

TABLE 1

Details of models

Model	Design C_L	Design ΔC_m	Maximum droop angle	Achieved C_L at design	Achieved ΔC_m ($C_L = 0$)	$(L/D)_{max}$	$C_{D_{min}}$
1	0	0.00852	29°	0.009	0.0048	7.40	0.0074
2	0.025	0.00852	51°	0.021	0.0078	7.80	0.0083
3	0.025	0.00670	33°	0.026	0.0028	8.05	0.0082
4	0.050	0.00487	38°	0.042	0.0050	8.35	0.0085
5	0	0.01157	50°	0.005	0.0085	7.30	0.0082
6	0	0.01157	50°	0.003	0.0094	7.35	0.0077
7	0	0.01364	60°	0.005	0.0115	7.35	0.0081
8	0.075	0.00304	44°	0.066	0.0022	8.50	0.0095
Symmetrical	0	0	0°	0	0.0002	7.55	0.0073

Printed in England for Her Majesty's Stationery Office by the Royal Aircraft Establishment, Farnborough. K.T.80.K.4.

℄ CHORD = 27 INS.
SEMI-SPAN = 5·633 INS.

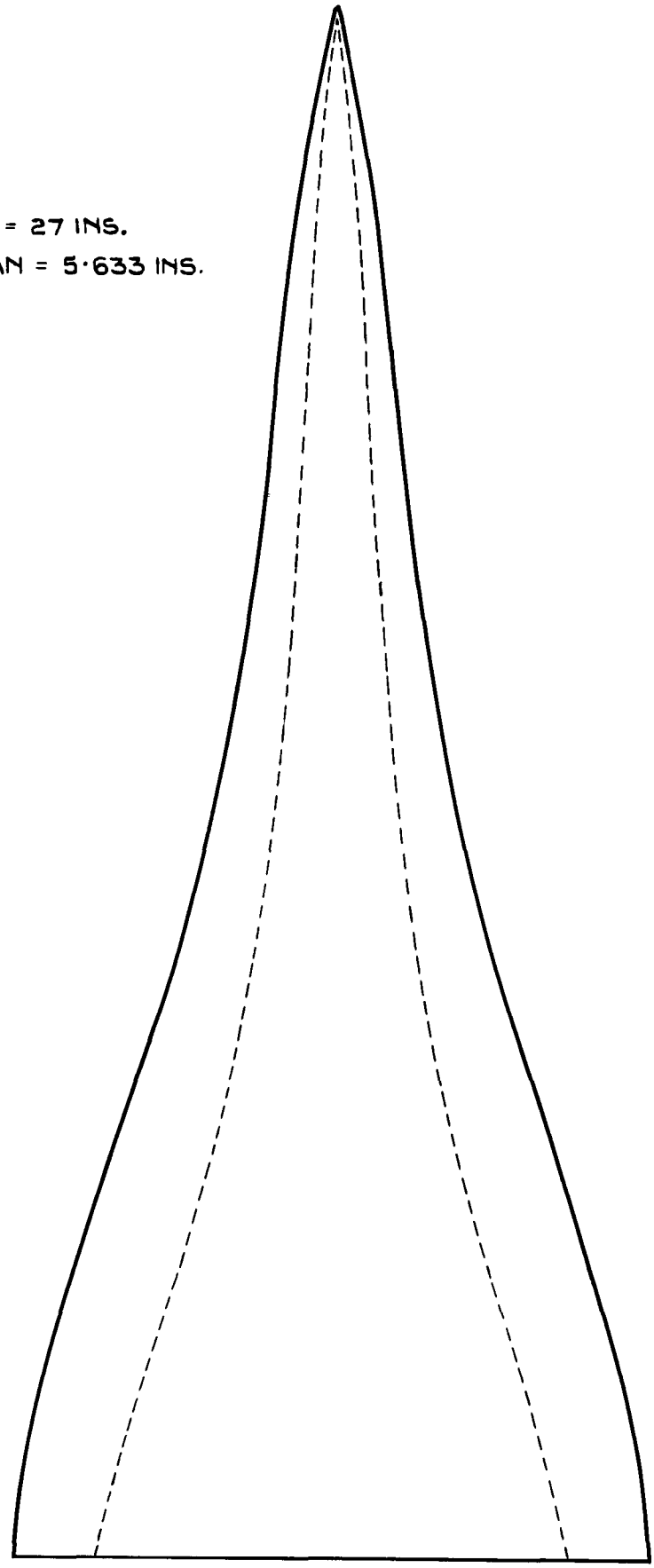

EQUATION OF LEADING EDGE $S(x) = S_T x \left(1{\cdot}2 - 2{\cdot}4x + 2{\cdot}2x^2 + 3x^3 - 3x^4\right)$

EQUATION OF SHOULDER LINE $\eta_0(x) = 0{\cdot}5, \quad x \leq 0{\cdot}5$

$= 0{\cdot}5 + (x - 0{\cdot}5)^2, \quad x \geq 0{\cdot}5$

FIG. 1. DETAILS OF MODEL PLANFORM

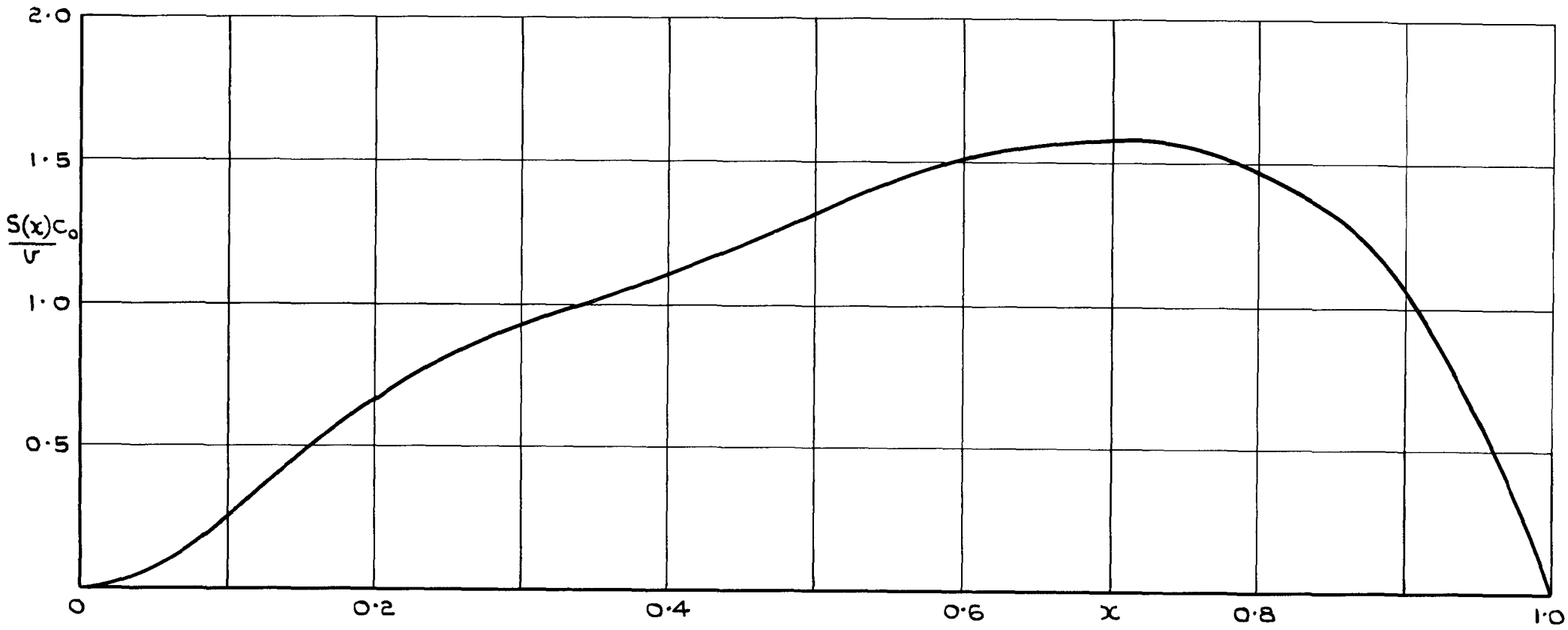

FIG. 2. CROSS – SECTIONAL AREA DISTRIBUTION

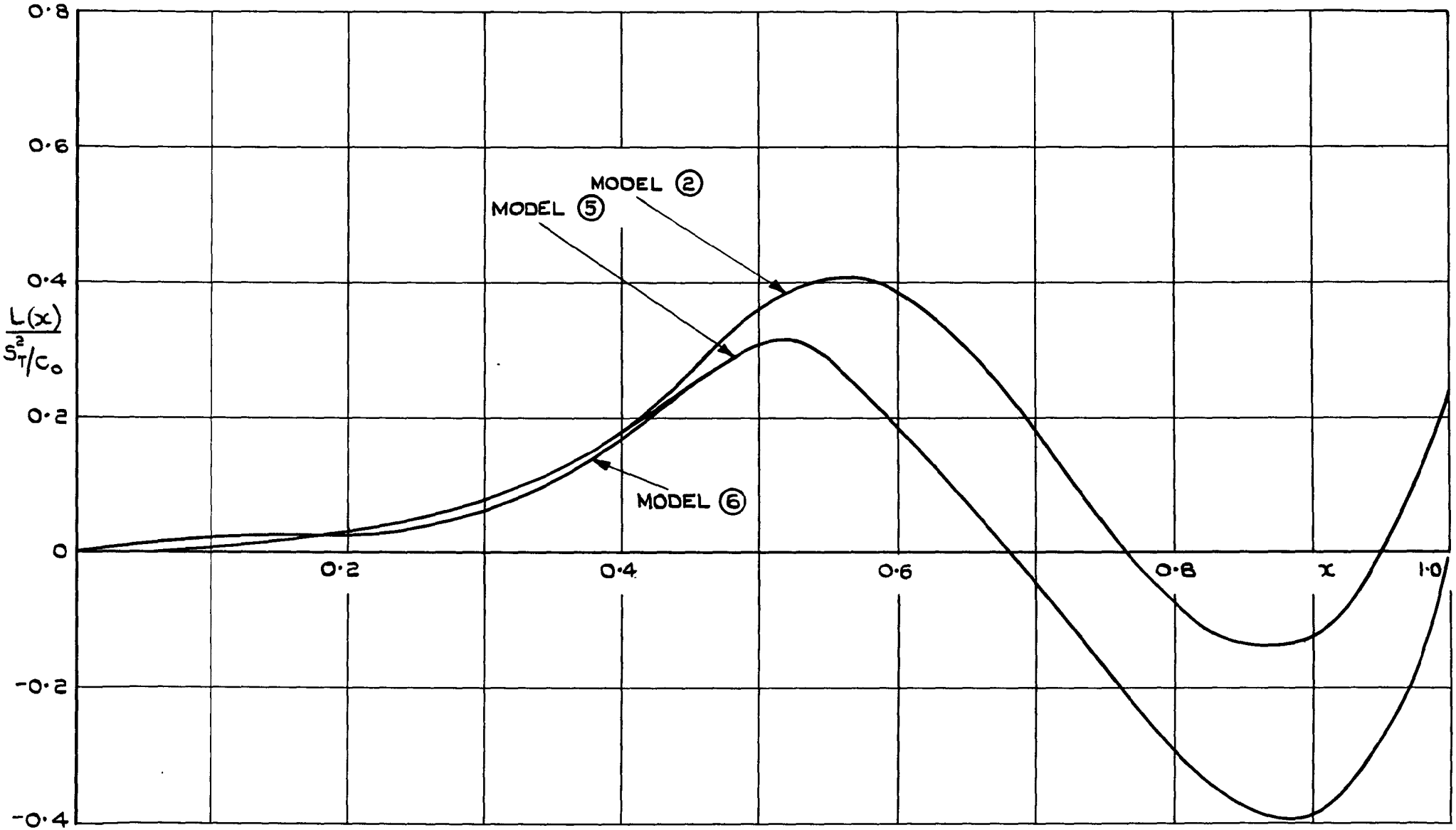

FIG. 3.(a) CHORDWISE VARIATION OF CROSS-LOAD

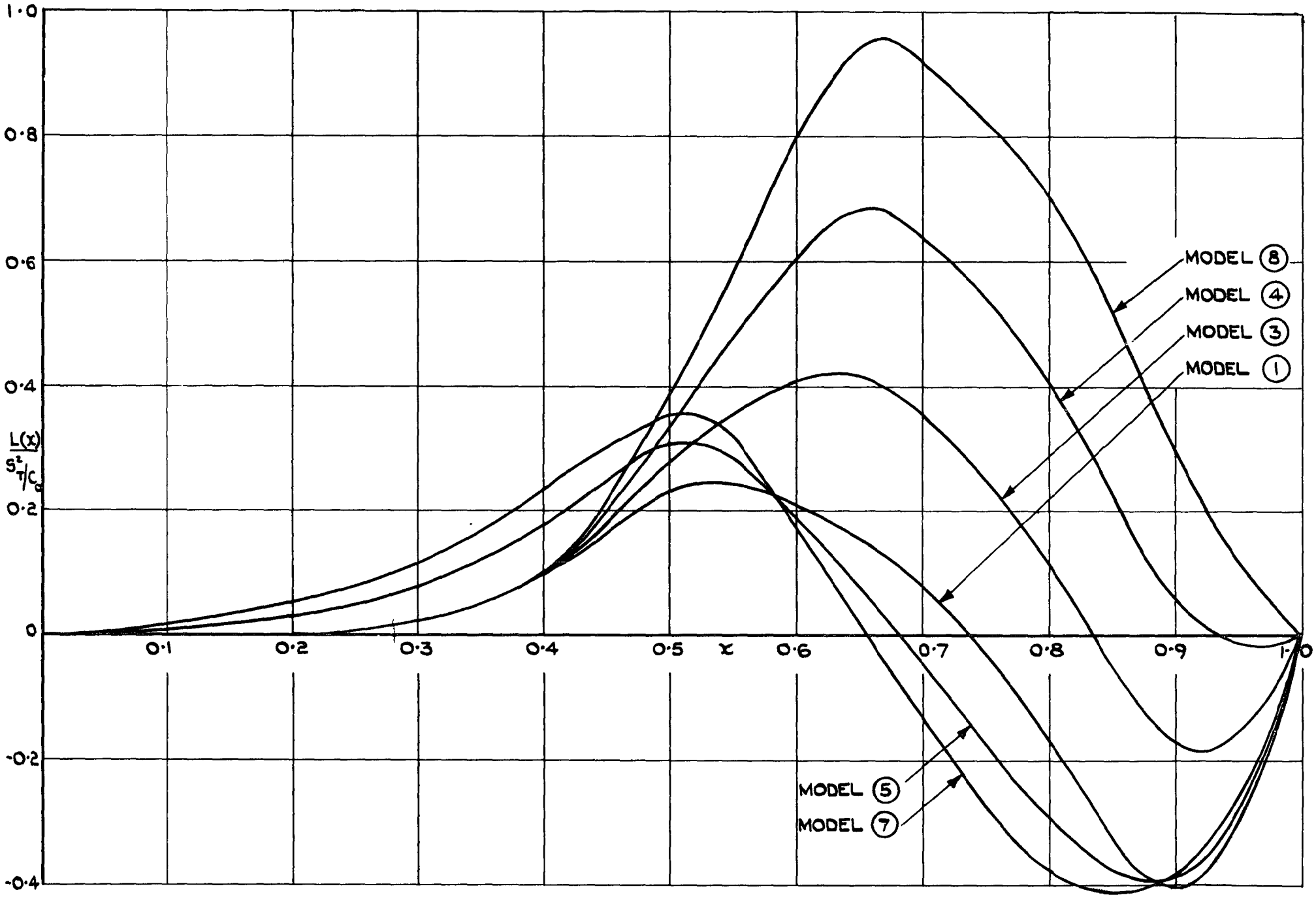

FIG. 3.(b) CHORDWISE VARIATION OF CROSS-LOAD

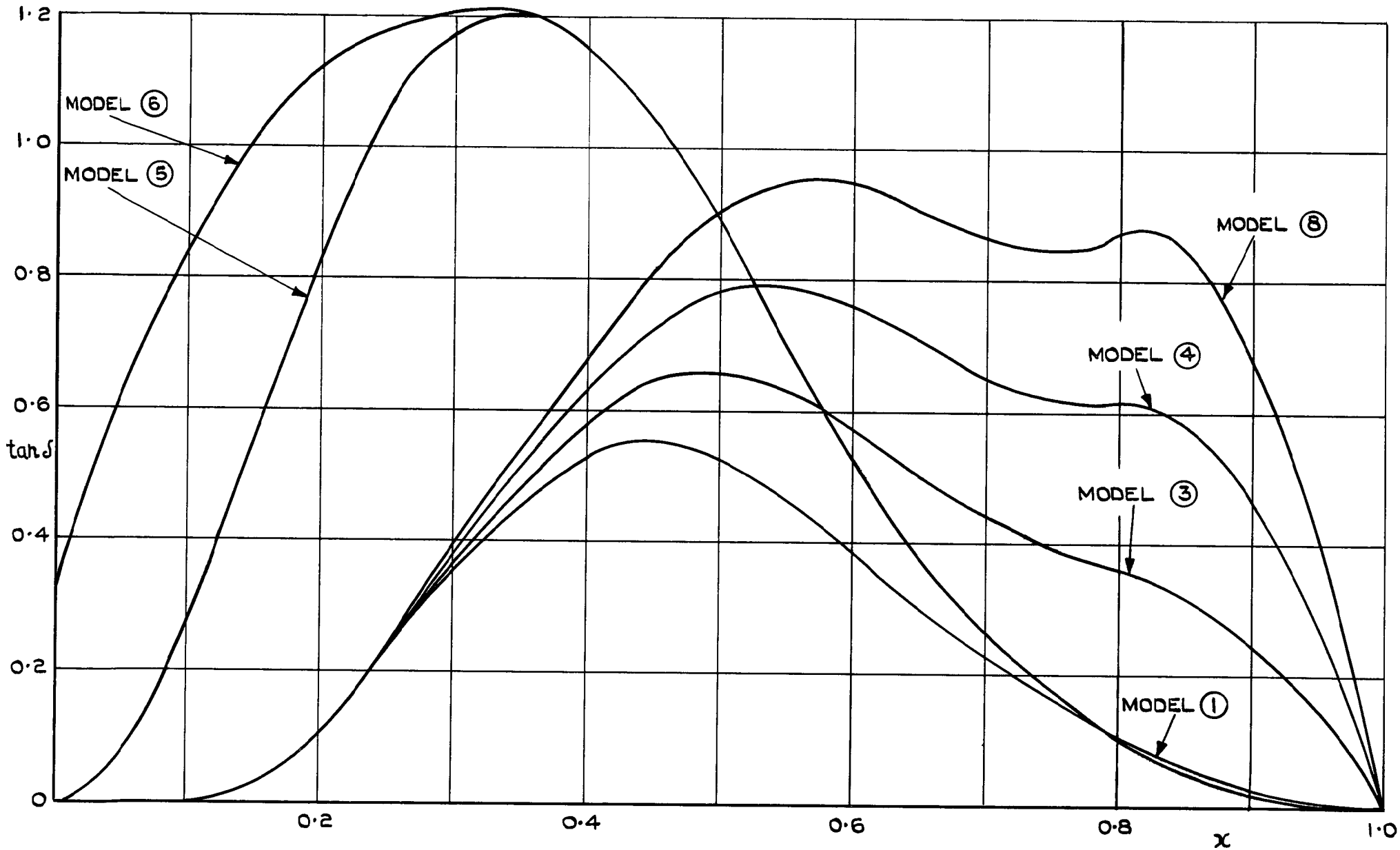

FIG. 4. (a) CHORDWISE VARIATION OF LEADING – EDGE DROOP ANGLE

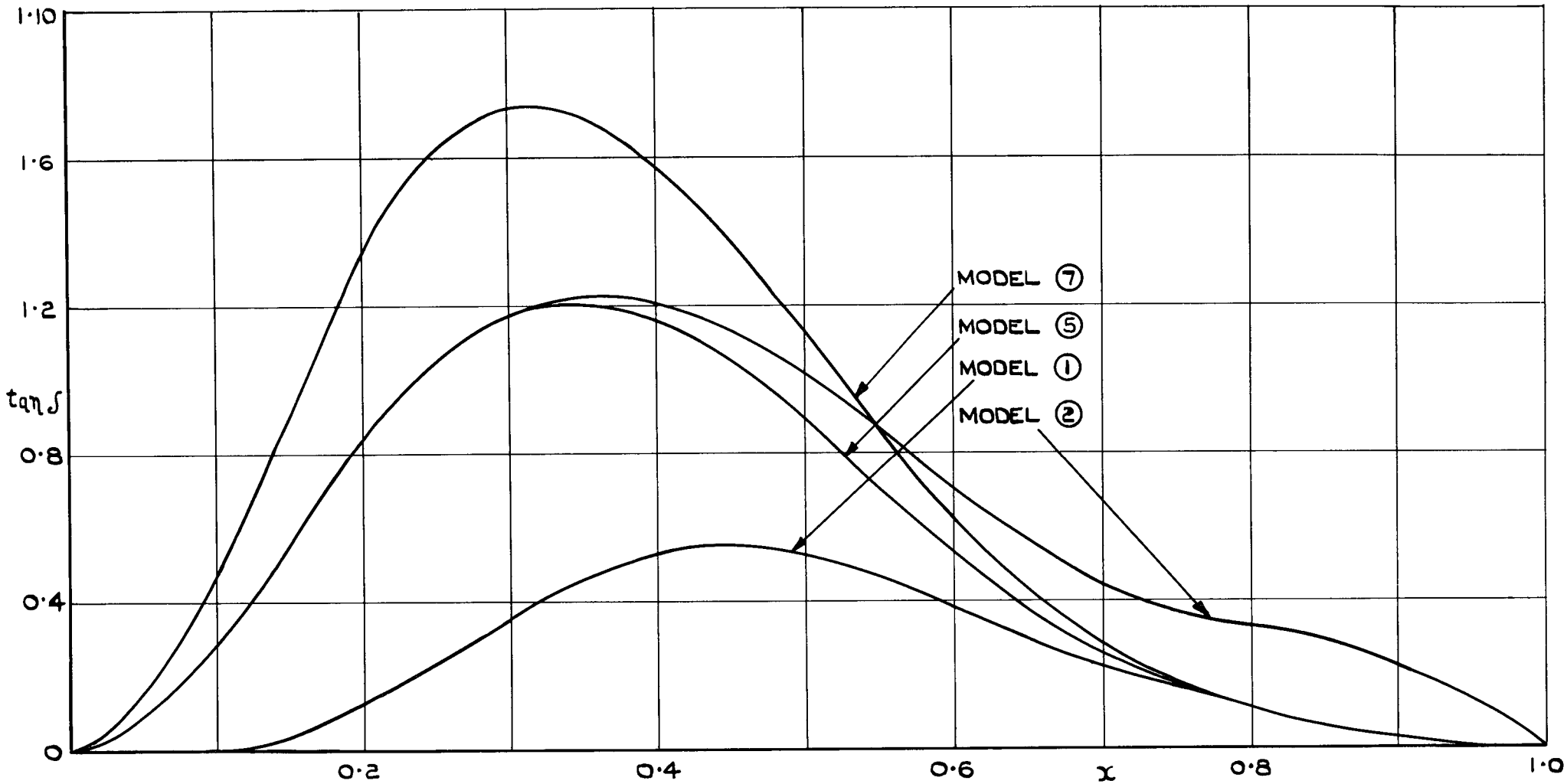

FIG. 4.(b) CHORDWISE VARIATION OF LEADING – EDGE DROOP ANGLE

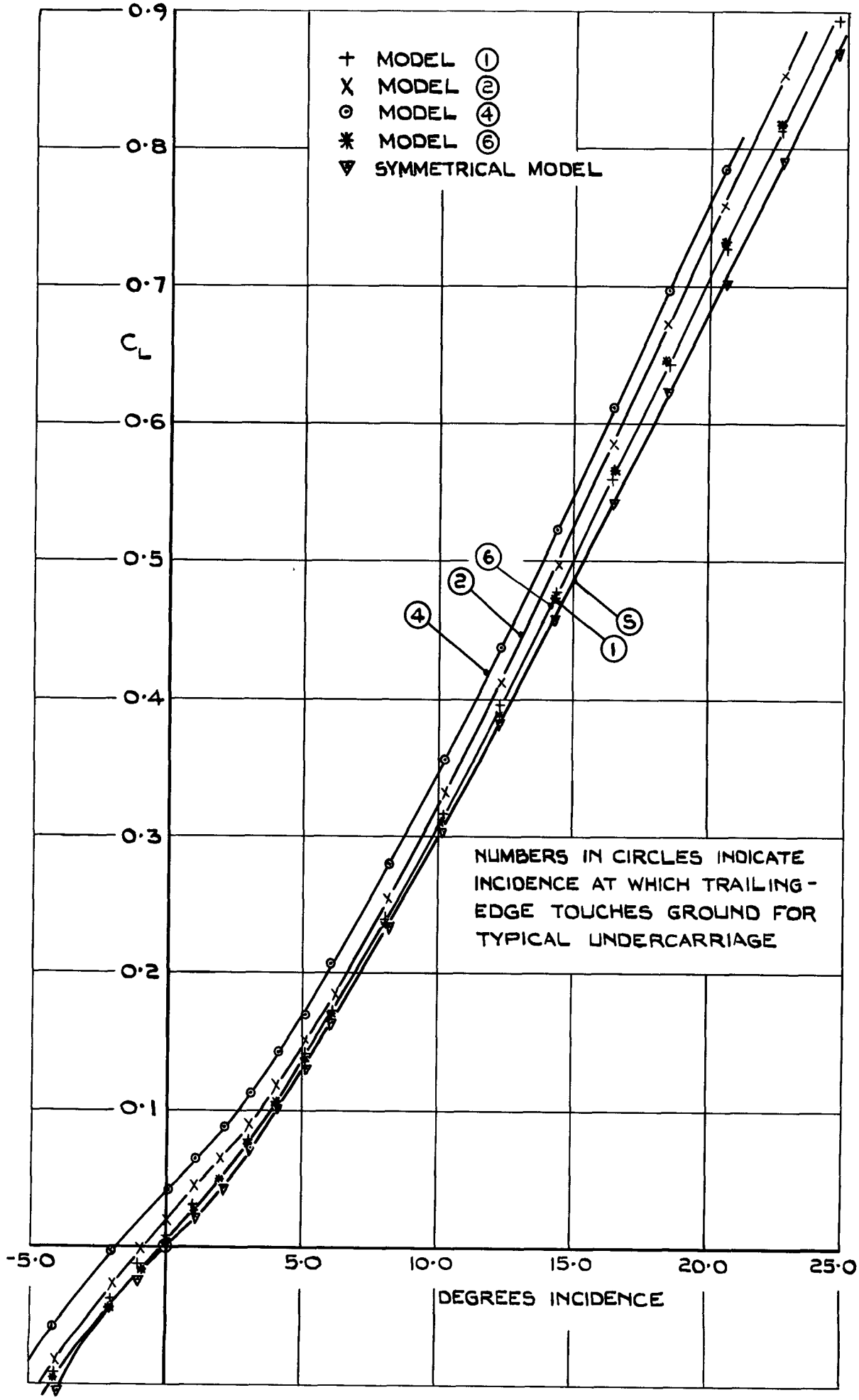

FIG. 5 (a) VARIATION OF LIFT WITH INCIDENCE

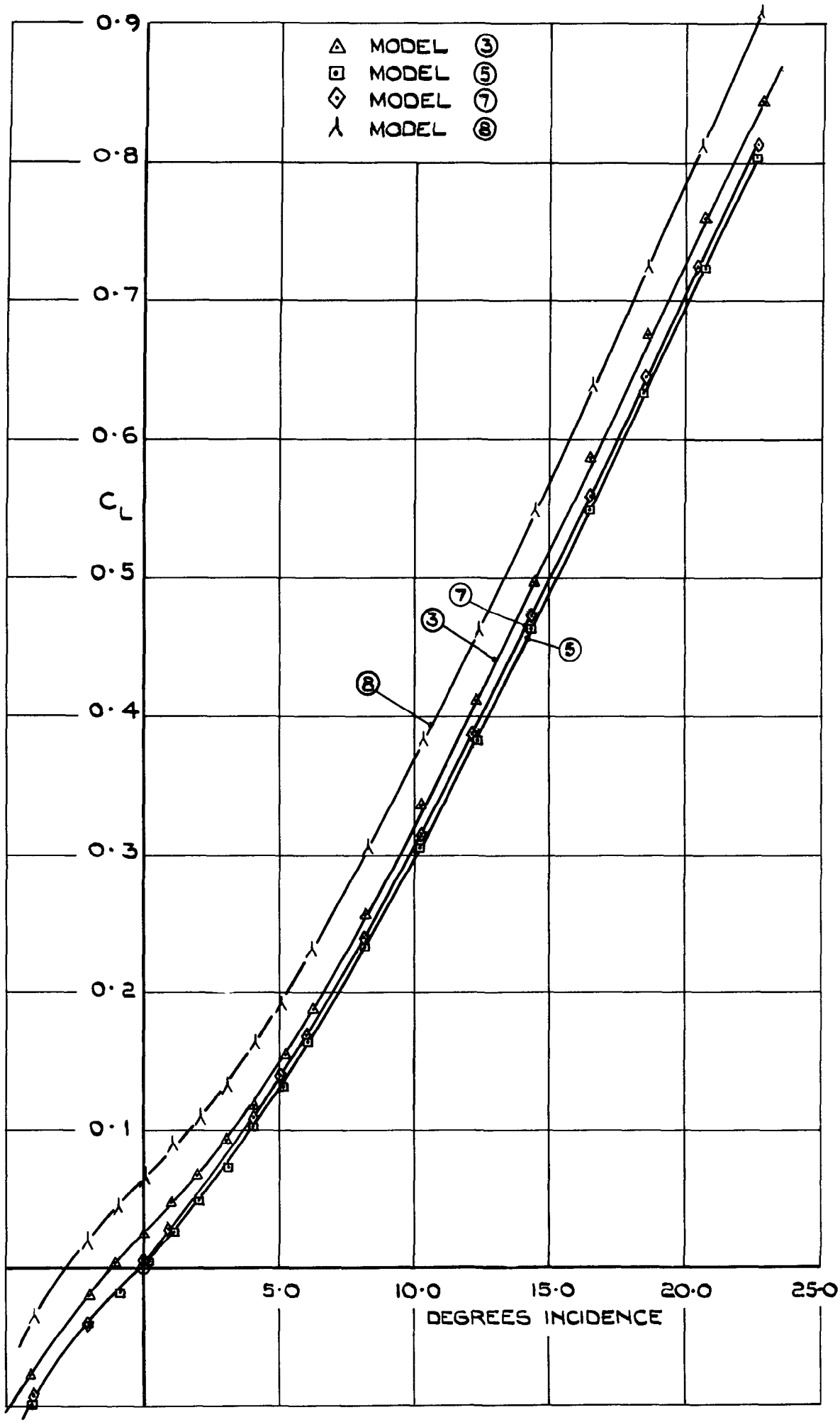

FIG. 5. (b) VARIATION OF LIFT WITH INCIDENCE

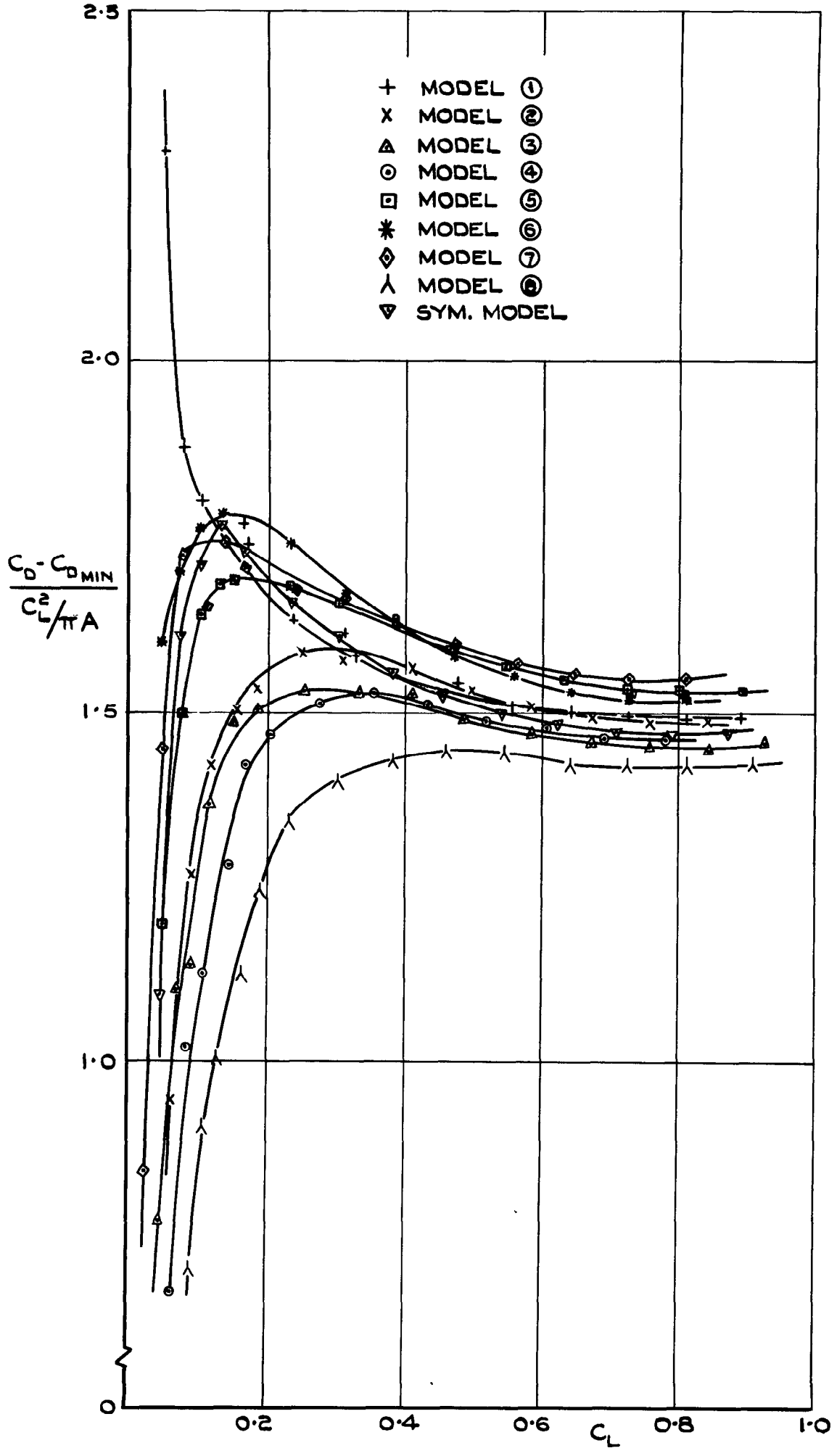

FIG. 6. VARIATION OF INDUCED DRAG FACTOR K WITH LIFT

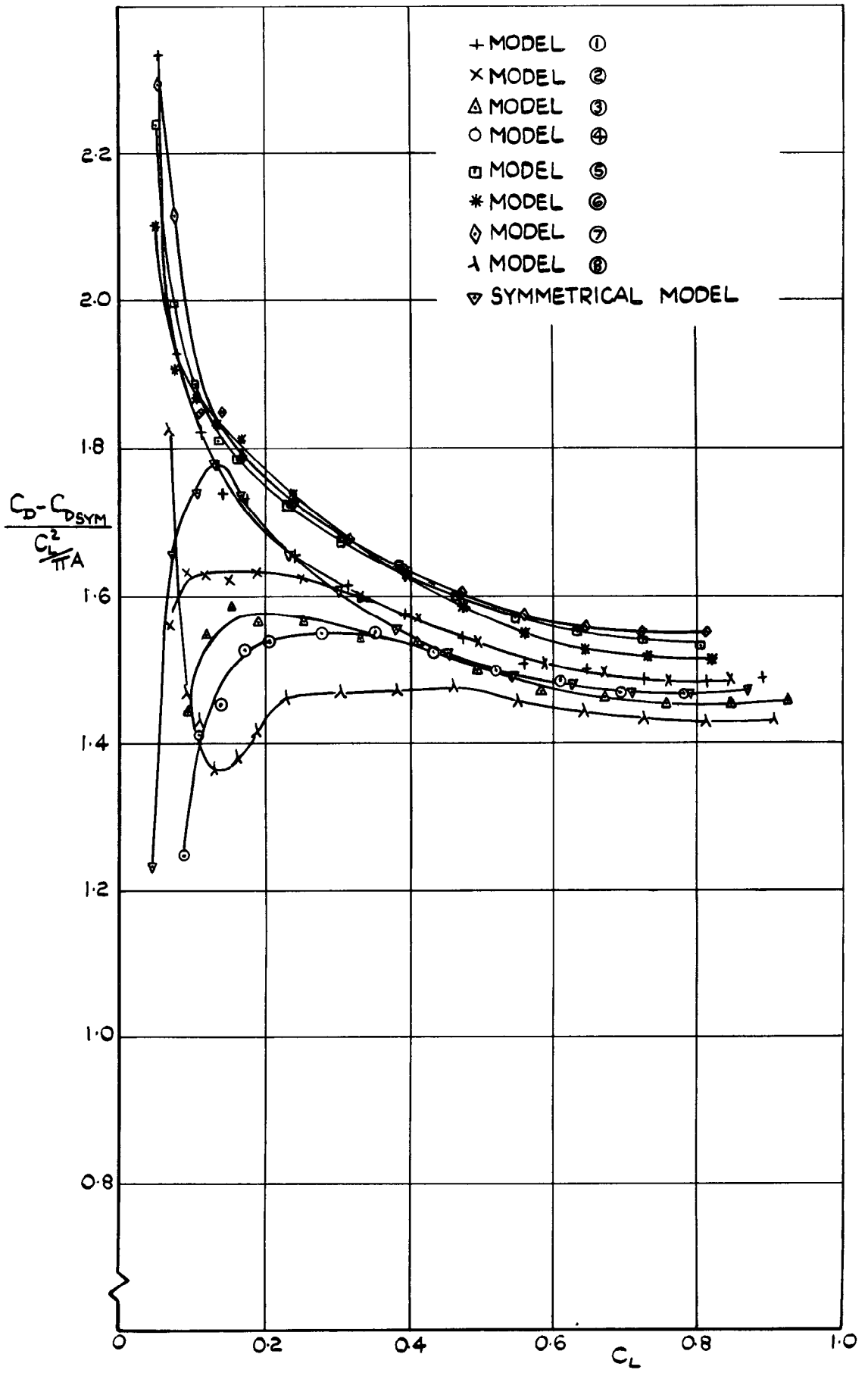

FIG. 7. VARIATION OF INDUCED DRAG FACTOR K_S WITH LIFT.

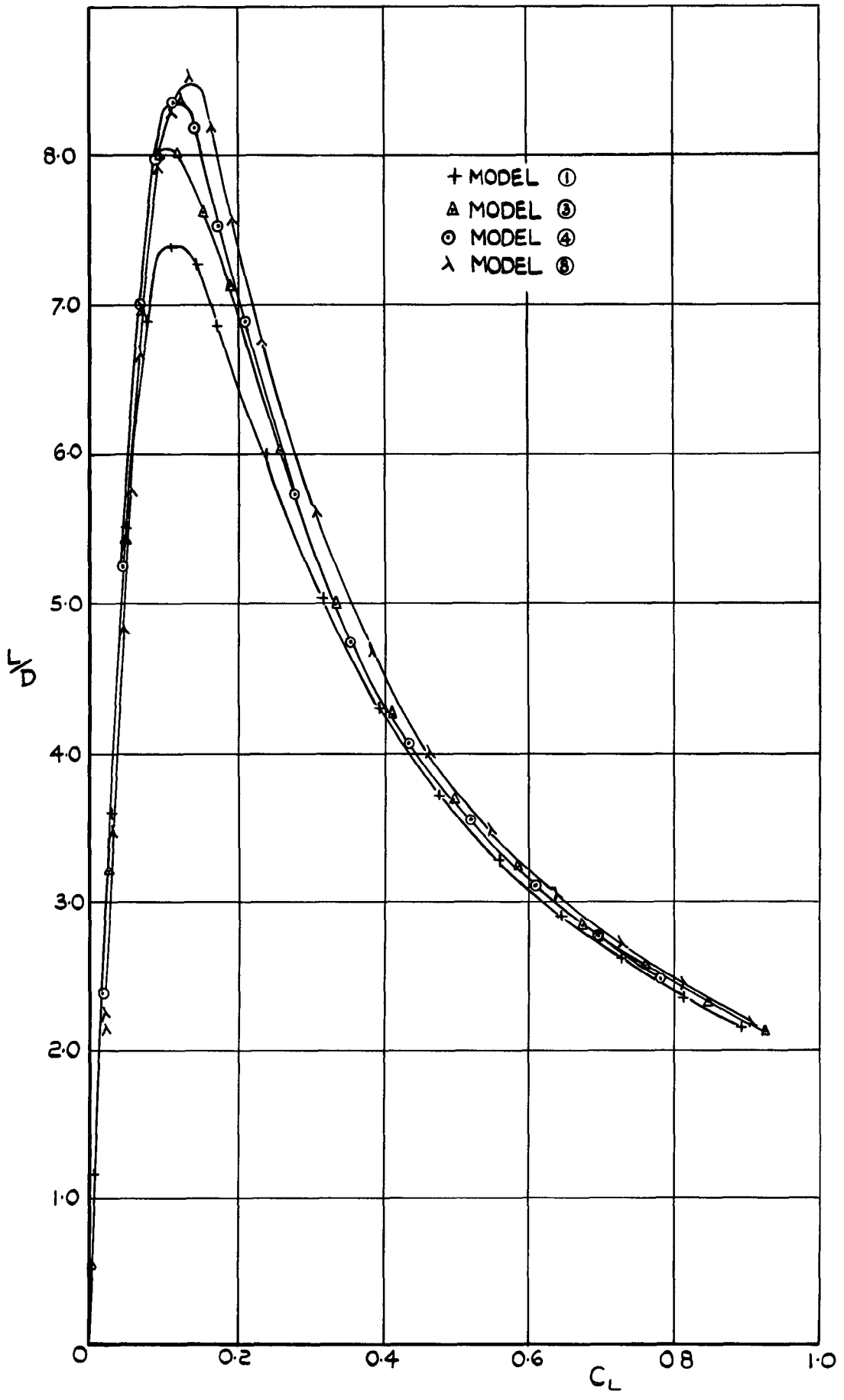

FIG. 8(a) VARIATION OF $^{L}/_{D}$ WITH LIFT.

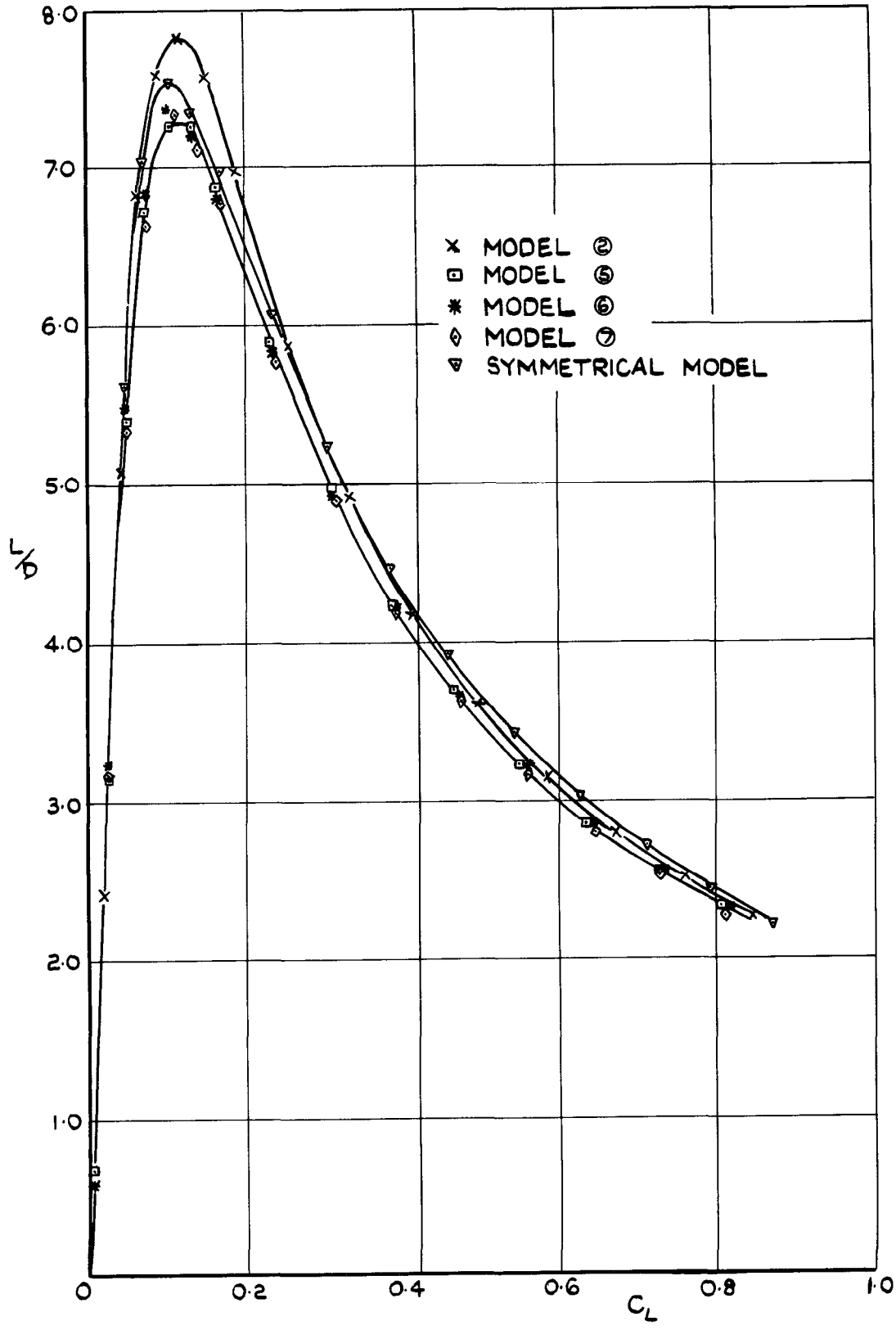

FIG. 8.(b) VARIATION OF $^{L}/_{D}$ WITH LIFT.

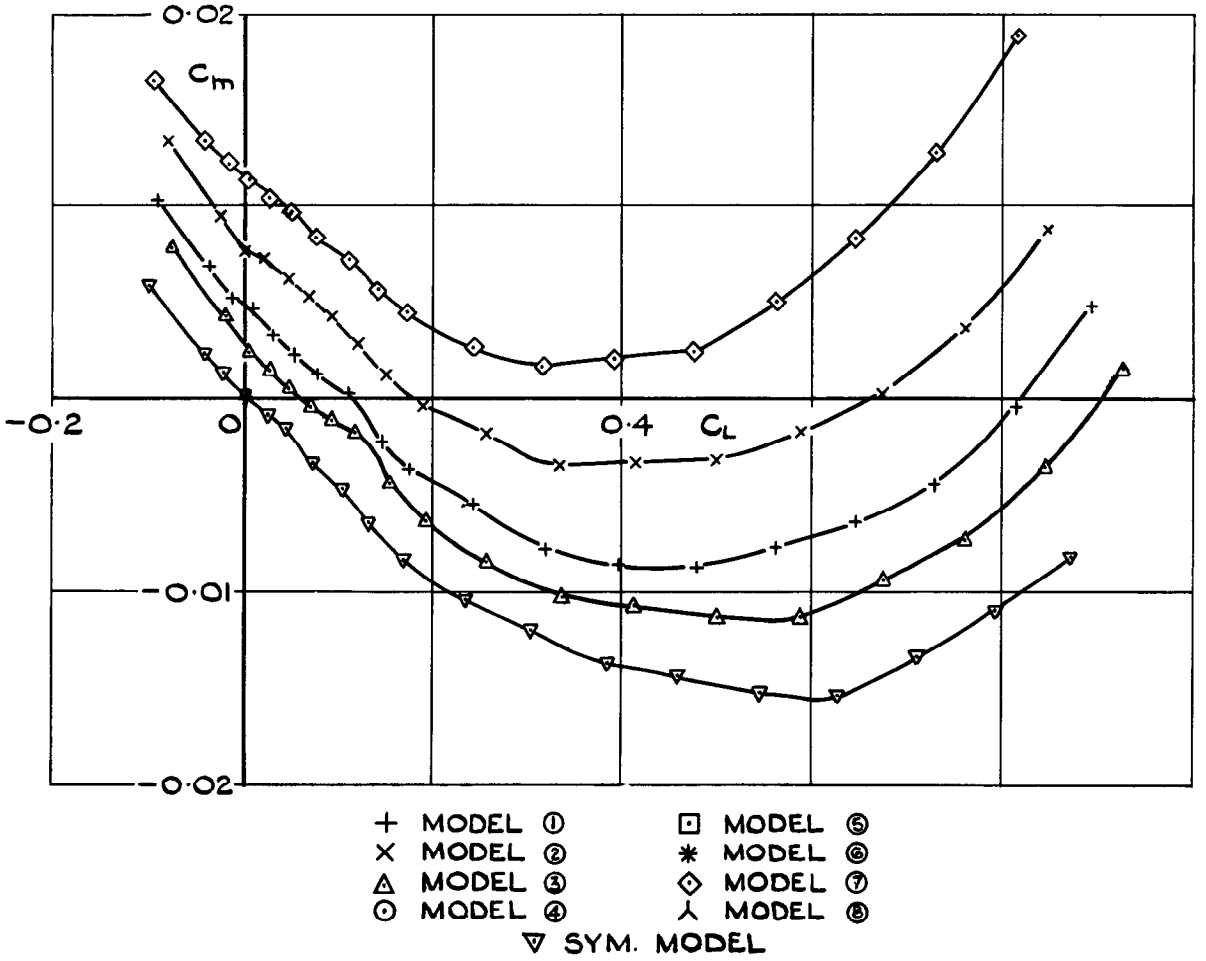

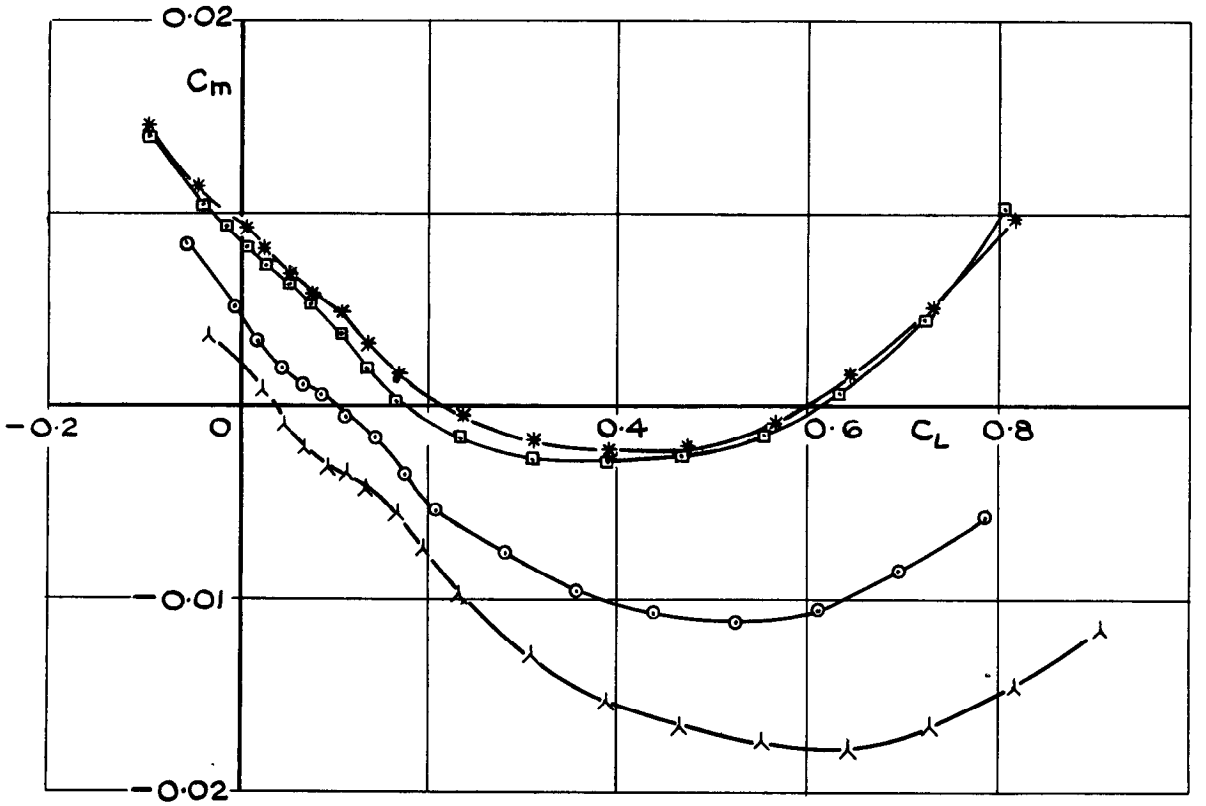

FIG.9. VARIATION OF PITCHING MOMENT WITH LIFT

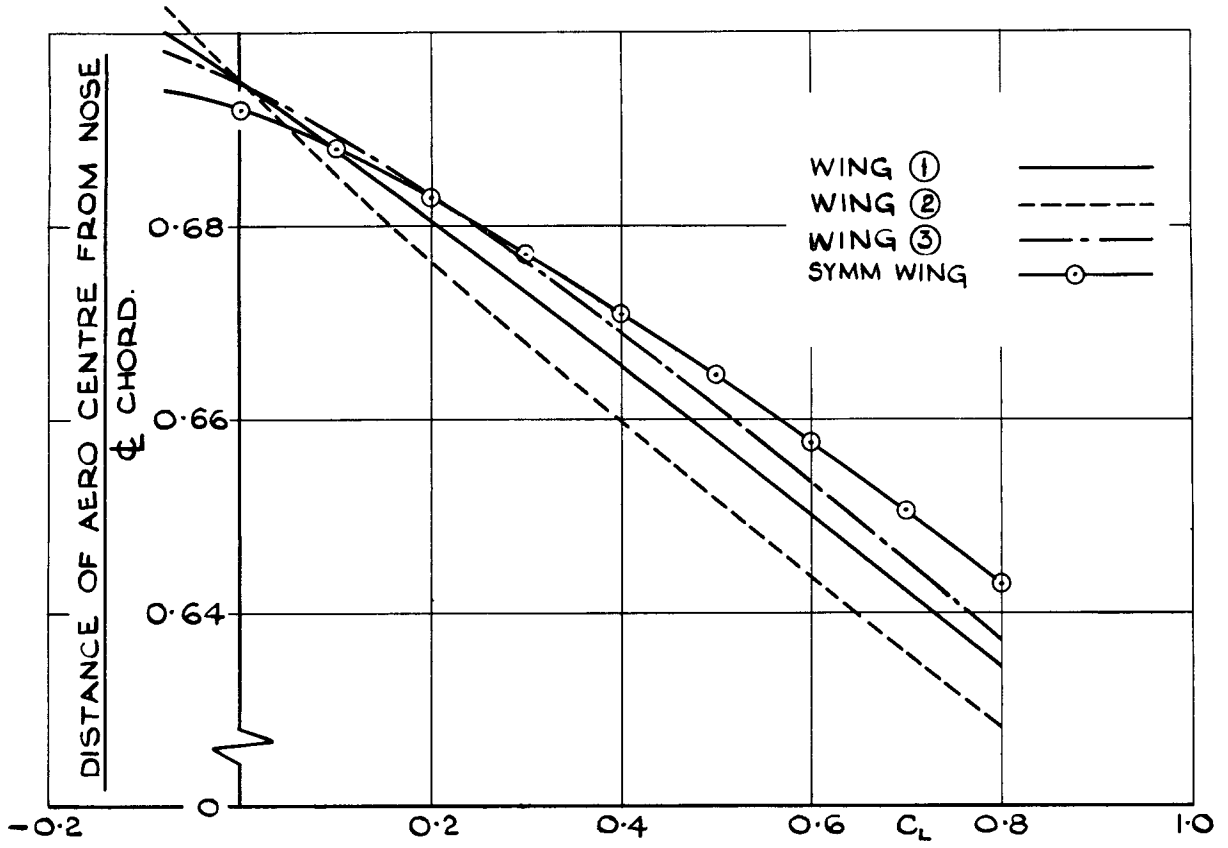

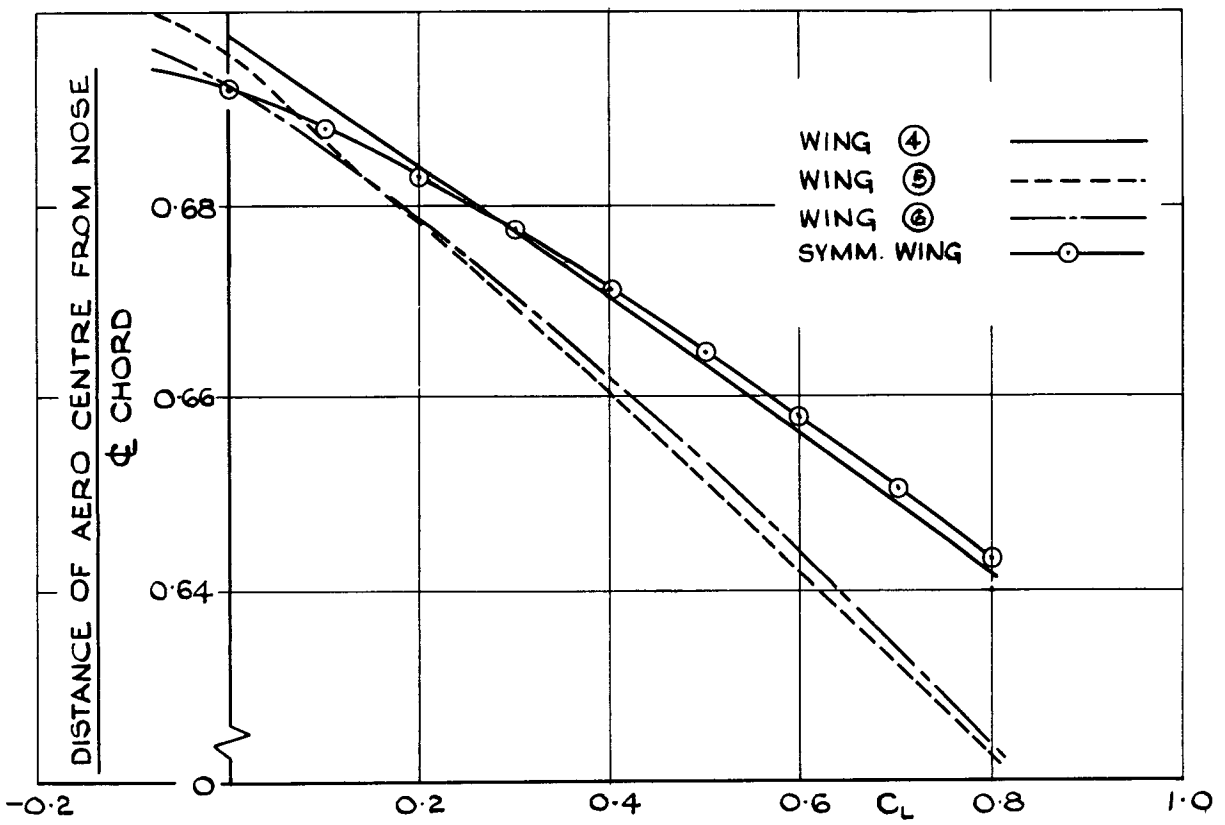

FIG. 10(a) VARIATION OF POSITION OF AERODYNAMIC CENTRE

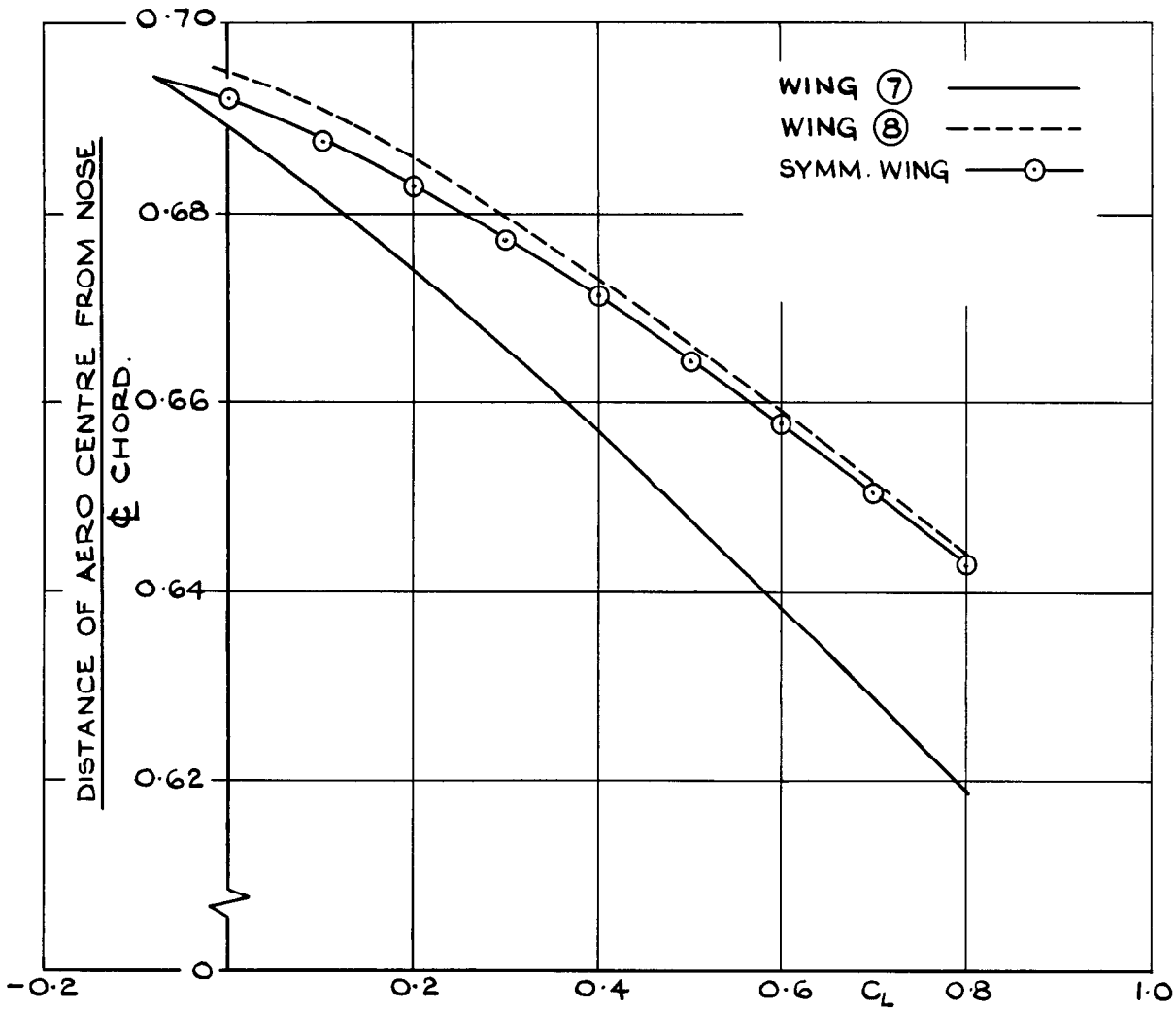

FIG 10(b) VARIATION OF POSITION OF AERODYNAMIC CENTRE

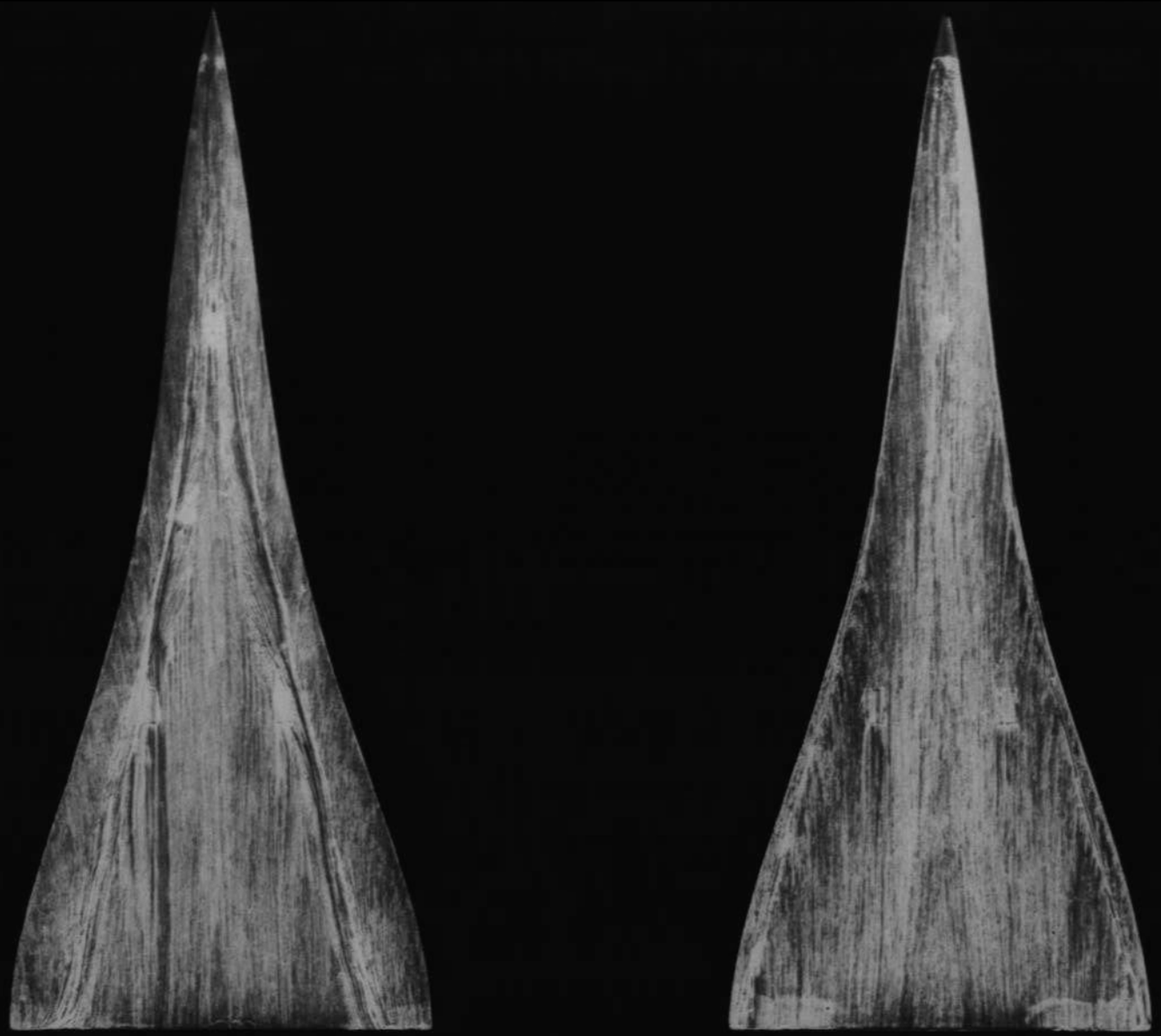

a. WITHOUT TRANSITION WIRES

b. WITH TRANSITION WIRES

FIG.11a & b. SURFACE FLOW PATTERNS FOR MODEL 6 AT DESIGN INCIDENCE WITH AND WITHOUT TRANSITION WIRES

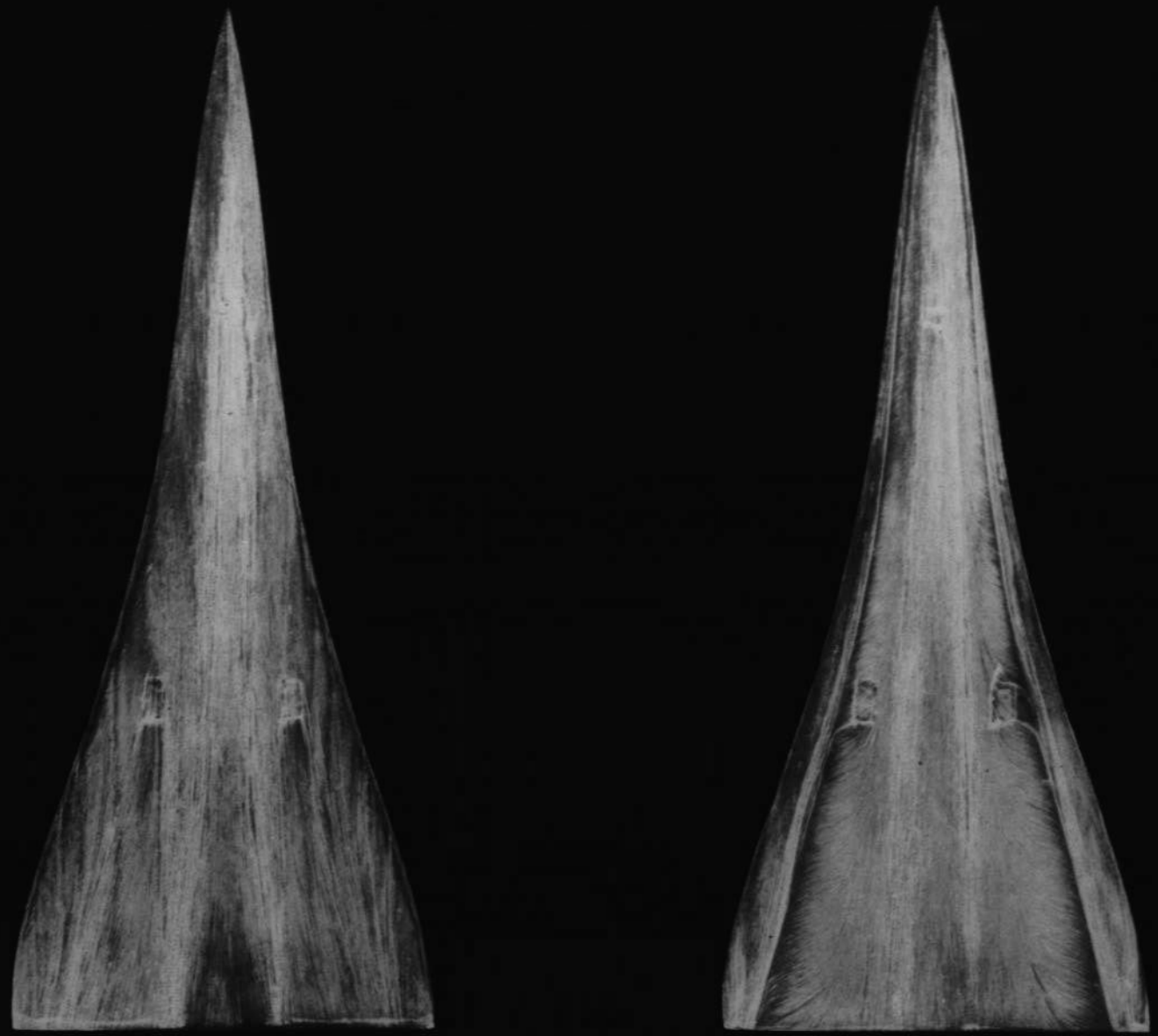

a. 2·5° INCIDENCE

b. 10° INCIDENCE

FIG.12a & b. SURFACE FLOW PATTERNS FOR MODEL 4 AT 2·5° AND AT 10° ABOVE DESIGN INCIDENCE

A.R.C. C.P. No.775

533.6.055:
533.6.071:
533.693.4

LOW-SPEED WIND-TUNNEL TESTS ON A SERIES OF CAMBERED OGEE WINGS. Earnshaw, P. B. November 1963.

A series of nine cambered ogee models, each having the same planform and area distribution, has been tested at low speeds. The camber variants have been designed by means of slender-wing theory and include variations both of lift coefficient for attached flow and of pitching moment at a given lift. For all wings, the flow development was regular regardless of load distribution except at low incidences, where the flow was very sensitive to defects in the leading edges. Trailing-edge effects dominated the load distribution achieved in the attachment condition; when an appreciable

(Over)

A.R.C. C.P. No.775

533.6.055:
533.6.071:
533.693.4

LOW-SPEED WIND-TUNNEL TESTS ON A SERIES OF CAMBERED OGEE WINGS. Earnshaw, P. B. November 1963.

A series of nine cambered ogee models, each having the same planform and area distribution, has been tested at low speeds. The camber variants have been designed by means of slender-wing theory and include variations both of lift coefficient for attached flow and of pitching moment at a given lift. For all wings, the flow development was regular regardless of load distribution except at low incidences, where the flow was very sensitive to defects in the leading edges. Trailing-edge effects dominated the load distribution achieved in the attachment condition; when an appreciable

(Over)

A.R.C. C.P. No.775

533.6.055:
533.6.071:
533.693.4

LOW-SPEED WIND-TUNNEL TESTS ON A SERIES OF CAMBERED OGEE WINGS. Earnshaw, P. B. November 1963.

A series of nine cambered ogee models, each having the same planform and area distribution, has been tested at low speeds. The camber variants have been designed by means of slender-wing theory and include variations both of lift coefficient for attached flow and of pitching moment at a given lift. For all wings, the flow development was regular regardless of load distribution except at low incidences, where the flow was very sensitive to defects in the leading edges. Trailing-edge effects dominated the load distribution achieved in the attachment condition; when an appreciable

(Over)

A.R.C. C.P. No.775

533.6.055:
533.6.071:
533.693.4

LOW-SPEED WIND-TUNNEL TESTS ON A SERIES OF CAMBERED OGEE WINGS. Earnshaw, P. B. November 1963.

A series of nine cambered ogee models, each having the same planform and area distribution, has been tested at low speeds. The camber variants have been designed by means of slender-wing theory and include variations both of lift coefficient for attached flow and of pitching moment at a given lift. For all wings, the flow development was regular regardless of load distribution except at low incidences, where the flow was very sensitive to defects in the leading edges. Trailing-edge effects dominated the load distribution achieved in the attachment condition; when an appreciable

(Over)

part of the load was carried over the forward part of the wing, correspondence between theory and experiment was reasonable. Increase of lift coefficient for attached flow had favourable effects with regard to both $(L/D)_{max}$ and the rate of forward movement of aerodynamic centre with increasing lift.

part of the load was carried over the forward part of the wing, correspondence between theory and experiment was reasonable. Increase of lift coefficient for attached flow had favourable effects with regard to both $(L/D)_{max}$ and the rate of forward movement of aerodynamic centre with increasing lift.

part of the load was carried over the forward part of the wing, correspondence between theory and experiment was reasonable. Increase of lift coefficient for attached flow had favourable effects with regard to both $(L/D)_{max}$ and the rate of forward movement of aerodynamic centre with increasing lift.

part of the load was carried over the forward part of the wing, correspondence between theory and experiment was reasonable. Increase of lift coefficient for attached flow had favourable effects with regard to both $(L/D)_{max}$ and the rate of forward movement of aerodynamic centre with increasing lift.

Published by
HER MAJESTY'S STATIONERY OFFICE

To be purchased from
York House, Kingsway, London W.C.2
423 Oxford Street, London W.1
13A Castle Street, Edinburgh 2
109 St. Mary Street, Cardiff
39 King Street, Manchester 2
50 Fairfax Street, Bristol 1
35 Smallbrook, Ringway, Birmingham 5
80 Chichester Street, Belfast 1
or through any bookseller

C.P. No. 775

S.O. CODE No. 23-9015-75